

# Screening of candidate substrates and coupling ions of transporters by thermostability shift assays

Homa Majd<sup>1†</sup>, Martin S King<sup>1†</sup>, Shane M Palmer<sup>1</sup>, Anthony C Smith<sup>1</sup>, Liam DH Elbourne<sup>2</sup>, Ian T Paulsen<sup>2</sup>, David Sharples<sup>3,4</sup>, Peter JF Henderson<sup>3,4</sup>, Edmund RS Kunji<sup>1\*</sup>

<sup>1</sup>Medical Research Council Mitochondrial Biology Unit, University of Cambridge, Cambridge, United Kingdom; <sup>2</sup>Department of Molecular Sciences, Macquarie University, Sydney, Australia; <sup>3</sup>Astbury Centre for Structural Molecular Biology, University of Leeds, Leeds, United Kingdom; <sup>4</sup>School of Biomedical Sciences, University of Leeds, Leeds, United Kingdom

**Abstract** Substrates of most transport proteins have not been identified, limiting our understanding of their role in physiology and disease. Traditional identification methods use transport assays with radioactive compounds, but they are technically challenging and many compounds are unavailable in radioactive form or are prohibitively expensive, precluding large-scale trials. Here, we present a high-throughput screening method that can identify candidate substrates from libraries of unlabeled compounds. The assay is based on the principle that transport proteins recognize substrates through specific interactions, which lead to enhanced stabilization of the transporter population in thermostability shift assays. Representatives of three different transporter (super)families were tested, which differ in structure as well as transport and ion coupling mechanisms. In each case, the substrates were identified correctly from a large set of chemically related compounds, including stereo-isoforms. In some cases, stabilization by substrate binding was enhanced further by ions, providing testable hypotheses on energy coupling mechanisms.

DOI: <https://doi.org/10.7554/eLife.38821.001>

\*For correspondence:  
ek@mrc-mbu.cam.ac.uk

†These authors contributed  
equally to this work

**Competing interests:** The  
authors declare that no  
competing interests exist.

**Funding:** See page 13

**Received:** 11 July 2018

**Accepted:** 11 October 2018

**Published:** 15 October 2018

**Reviewing editor:** Volker  
Dötsch, J.W. Goethe-University,  
Germany

© Copyright Majd et al. This  
article is distributed under the  
terms of the [Creative Commons  
Attribution License](#), which  
permits unrestricted use and  
redistribution provided that the  
original author and source are  
credited.

## Introduction

Transport proteins, also called transporters, porters, carriers, translocases or permeases, encompass a diverse and ubiquitous group of membrane proteins that facilitate the translocation of ions and molecules across all types of biological membranes, linking biochemical pathways, maintaining homeostasis and providing building blocks for growth and maintenance. They comprise 5–15% of the genomic complement in most organisms. Transport proteins are classified into four major groups: primary active transporters, secondary active transporters, facilitative transporters, and channels. Human solute transport proteins have been divided into 65 subfamilies (based on sequence alignments or experimentally determined substrate specificities), which transport a diverse range of compounds, including amino acids, sugars, nucleotides, lipids, vitamins, hormones, inorganic and organic ions, metals, xenobiotics and drugs (<http://slc.bioparadigms.org/>). Of the 538 identified solute transport proteins in humans, more than a quarter have no assigned substrate specificity (<http://slc.bioparadigms.org/>). Consequently, their role in human physiology is ill-defined and opportunities for drug intervention are missed (*Hediger et al., 2013*). Currently, about half of the transport proteins have been associated with human disease (*Rask-Andersen et al., 2013*; *Hediger et al., 2013*; *Lin et al., 2015*), but only 12 classes of drugs target them directly, despite

their inherent 'druggability' (Hediger *et al.*, 2013; Lin *et al.*, 2015; César-Razquin *et al.*, 2015; Fauman *et al.*, 2011). The situation is not better in other eukaryotic organisms and bacterial pathogens, currently on the WHO list (Supplementary file 1) (Elbourne *et al.*, 2017). For most transporters in the sequence databases, the identifications are preliminary because they are based only on sequence homology without direct experimental evidence for the substrates, even though single amino acid residue variations in the substrate binding site can alter the specificity profoundly. Moreover, the substrate specificities of some transporters may have been incompletely or incorrectly assigned. Finally, there could be membrane proteins with unassigned function that belong to unidentified transporter families, which are not counted at all.

One of the major challenges is to find the correct substrates from a large number of potential candidates. There are approximately ~3,000 metabolites in *Escherichia coli* (Sajed *et al.*, 2016), ~16,000 in *Saccharomyces cerevisiae* (Ramirez-Gaona *et al.*, 2017), ~40,000 in *Homo sapiens* (Wishart *et al.*, 2013), and plants must have even more as they carry out an extensive secondary metabolism. Some metabolites, such as vitamin B<sub>6</sub>, have several interconvertible species, each of which could be transported. The classical method to identify transport proteins monitors the accumulation of radiolabeled compounds in whole cells, membrane vesicles or proteoliposomes. However, these experiments can easily fail when the expressed transporters are not active due to targeting, insertion or folding issues, when they are unstable in purification and reconstitution experiments, or when substrate and coupling ion gradients are not setup correctly. Moreover, some compounds are not available in radioactive form or are prohibitively expensive, preventing large-scale identification trials. Given all these technical difficulties, it is often necessary to limit the number of candidate substrates first by using phylogenetic analysis, by analyzing phenotypic (patho)physiological data, by complementation studies or by metabolic analysis of knock-out or mutant strains.

Therefore, there is an unmet demand for the development of new methods to limit the number of potential substrates for identification of solute carriers. Here, we present a high-throughput screening method for the identification of substrates of transporters, which does not require radioactive compounds or prior knowledge. The method uses the simple concept that transporters recognize their substrates through specific interactions, enhancing their stabilization in thermostability shift assays. We verify the approach by defining the substrate specificity of three solute carriers from different bacterial and eukaryotic protein families and show that these experiments also provide valuable clues about the ion coupling mechanism.

## Results

### Principle of the method

Ligands, such as substrates or inhibitors, are recognized by transport proteins through specific interactions at the exclusion of other molecules. The formation of these additional bonds leads to an increase in the total number of interactions (Robinson and Kunji, 2006; Yan, 2017; Yamashita *et al.*, 2005). Consequently, binding leads to an overall increase in the stability of the ligand-bound species compared to the unliganded species in the population of protein molecules. We have previously shown that the mitochondrial ADP/ATP carrier (AAC) from the thermophilic fungus *Thermothelomyces thermophila* (UniProt G2QNH0) when purified in dodecyl-maltoside is stabilized upon binding of its specific inhibitors carboxyatractyloside and bongkreikic acid in thermostability shift assays using the thiol-reactive fluorophore N-[4-(7-diethylamino-4-methyl-3-coumarinyl)-phenyl]-maleimide (CPM) (Crichton *et al.*, 2015; King *et al.*, 2016). In the assay, the apparent melting temperature  $T_m$  of a population of purified transporters is determined by monitoring the increase in fluorescence by CPM reacting with thiols that have become exposed due to thermal denaturation of the proteins (Figure 1a). The apparent melting temperature  $T_m$  is the temperature at which the rate of unfolding for a given population is highest. We tested whether transported substrates can also cause a shift in thermostability, as their properties differ quite substantially from those of inhibitors or other tight binders. Indeed, the thermostability of the AAC population was enhanced in the presence of ADP and ATP, but not in the presence of AMP, which reflects the known substrate specificity of the carrier well (Mifsud *et al.*, 2013) (Figure 1b). This effect is only observed at high concentrations of the substrate, well above the apparent  $K_m$  of transport (Figure 1—figure supplement 1). The higher the substrate concentration, the higher the likelihood that

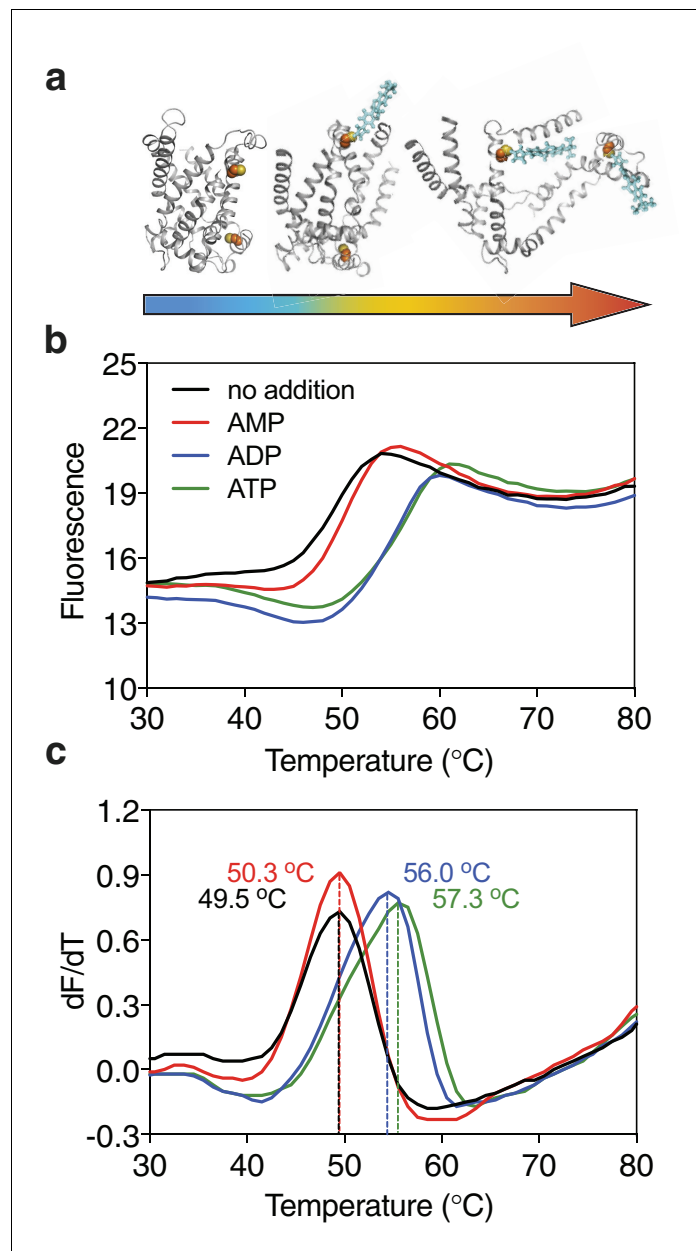


**Figure 1.** Substrate-induced stabilization of a mitochondrial ADP/ATP carrier. (a) As protein molecules in a population unfold due to a gradual rise in temperature (25–90°C), buried cysteine residues become solvent-exposed and accessible to the thiol-specific probe CPM (blue stick representation) that becomes fluorescent upon reaction. (b) Typical unfolding curves of the mitochondrial ADP/ATP carrier of *Thermothelomyces thermophila* (2 µg) in the absence and presence of 2.5 mM AMP, ADP and ATP, shown in red, blue and green, respectively. (c) The apparent melting temperature ( $T_m$ ) is the peak in the derivative of the unfolding curve ( $dF/dT$ ), which is used as an indicator of thermal stability. The apparent melting temperatures reported in the text are from three independent protein purifications.

DOI: <https://doi.org/10.7554/eLife.38821.002>

The following figure supplement is available for figure 1:

**Figure supplement 1.** Substrate-induced stabilization of a mitochondrial ADP/ATP carrier.

DOI: <https://doi.org/10.7554/eLife.38821.003>

part of the population is prevented from unfolding by binding of the substrate, leading to the observed shift in thermostability. We reasoned that this approach could be applied as a screening method to find substrate candidates of uncharacterized transporters by using compound libraries. To verify the method, we have tested transporters from three different (super)families, which are distinct in structure and transport mechanism.

### Substrates cause specific thermostability shifts in different transporters

The galactose transporter GalP of *E. coli* (Henderson, 1977) is a prototypical member of the sugar porter family that belongs to the major facilitator superfamily (MFS) (Pao et al., 1998). Currently, the MFS contains 24 different transporter families and 320,665 sequence entries from 5224 species, but the substrates for the vast majority of them have not been formally identified (Pfam CL0015). In humans, 14 of the 65 solute carrier families belong to the MFS, and substrates are not known for around 12% of them (<http://slc.bioparadigms.org/>).

The structure of GalP has not been determined, but those of its mammalian homologs GLUT1 (Deng et al., 2014), GLUT3 (Deng et al., 2015), and GLUT5 (Nomura et al., 2015) are available (Figure 2a). GalP contains three cysteine residues, of which only one is readily accessible to reaction with *N*-ethylmaleimide (McDonald and Henderson, 2001). To evaluate the strategy, we measured the unfolding curves of purified GalP in dodecyl-maltoside in the presence of a large number of different sugars. We determined the temperature shift by subtracting the apparent  $T_m$  of unliganded GalP ( $57.6 \pm 0.3^\circ\text{C}$ ) from the apparent  $T_m$  values observed in the presence of compounds ( $\Delta T_m$ ). The GalP population was markedly stabilized by D-glucosamine ( $\Delta T_m$ ;  $5.7 \pm 0.4^\circ\text{C}$ ), D-glucose ( $\Delta T_m$ ;  $4.2 \pm 0.5^\circ\text{C}$ ), D-galactose ( $\Delta T_m$ ;  $2.1 \pm 0.6^\circ\text{C}$ ) (Figure 2—figure supplement 1), and to a lesser extent by D-talose, 2-deoxy-D-glucose, 6-deoxy-D-glucose. Importantly, the related L-isofamilies showed no significant shift (Figure 2b). These results match the known substrate specificity of GalP well (Henderson and Maiden, 1990; Walmsley et al., 1994). D-Glucosamine, the most stabilizing compound, had not been investigated previously, but transport assays showed that this compound is a new substrate (Figure 2—figure supplement 2), demonstrating that the assay can be used to discover as well as to extend the substrate specificity of transport proteins.

The transport protein Mhp1 from *Microbacterium liquefaciens* (UniProt D6R8X8) transports 5-substituted hydantoin in a sodium-coupled mechanism (Suzuki and Henderson, 2006; Shimamura et al., 2010) (Figure 2c), and is a member of the nucleobase-cation-symport family of homologous proteins that also transport purines, pyrimidines, vitamins and related metabolites. The transporter has the LeuT-fold (Shimamura et al., 2010; Yamashita et al., 2005) and belongs to the amino acid-polyamine-organocation superfamily (Västermark and Saier, 2014), which currently contains 20 families and 147,819 sequence entries, the substrates of which have mostly not been identified (Pfam CL0062). Mhp1 contains three cysteine residues, of which only one is readily accessible to reaction with *N*-ethylmaleimide (Calabrese et al., 2017). Purified Mhp1 in dodecyl-maltoside had an apparent  $T_m$  of  $51.3^\circ\text{C} \pm 0.6^\circ\text{C}$  and to test the binding specificity, the  $\Delta T_m$  was determined upon addition of different nucleobases and other compounds (Figure 2d). The only stabilizing compounds were 5-indolylmethyl-L-hydantoin ( $\Delta T_m$ ;  $14.1 \pm 1.2^\circ\text{C}$ ), 5-benzyl-L-hydantoin ( $\Delta T_m$ ;  $13.6 \pm 1.2^\circ\text{C}$ ) and 5-bromovinylhydantoin ( $\Delta T_m$ ;  $11.9 \pm 1.1^\circ\text{C}$ ) (Figure 2—figure supplement 3). A chemically related inhibitor of Mhp1, 5-(2-naphthylmethyl)-L-hydantoin (L-NMH) also led to a thermostability shift ( $\Delta T_m$ ;  $15.6 \pm 1.7^\circ\text{C}$ ) (Figure 2d). These results match the known substrate and inhibitor specificity of Mhp1 (Simmons et al., 2014), showing that the assay could identify substrates from a set of closely related compounds without false positives.

To validate the method further, we also screened the mitochondrial ADP/ATP carrier from *T. thermophila* (UniProt G2QNH0) (King et al., 2016) (Figure 2e). This transport protein belongs to the mitochondrial carrier family (MCF), which is involved in the translocation of chemically diverse compounds across the mitochondrial inner membrane, using uniport, symport or antiport modes of transport (Kunji, 2012). Currently, there are 89,340 different sequence entries from 831 different species in the database (Pfam PF00153). In humans, the MCF is the largest solute carrier family with 53 different members (SLC25), but the substrate specificity of only half of them has been defined (Kunji, 2012). We screened the thermostability of purified AAC using a library of mitochondrial compounds (Figure 2—figure supplement 4). In the presence of ATP, ADP, and dADP the population was stabilized, showing  $\Delta T_m$  values of  $7.2 \pm 0.2$ ,  $6.0 \pm 0.5$  and  $1.8 \pm 0.2^\circ\text{C}$ , respectively (Figures 1b and 2f). Some other compounds, mostly structurally related nucleotides, also stabilized the protein,

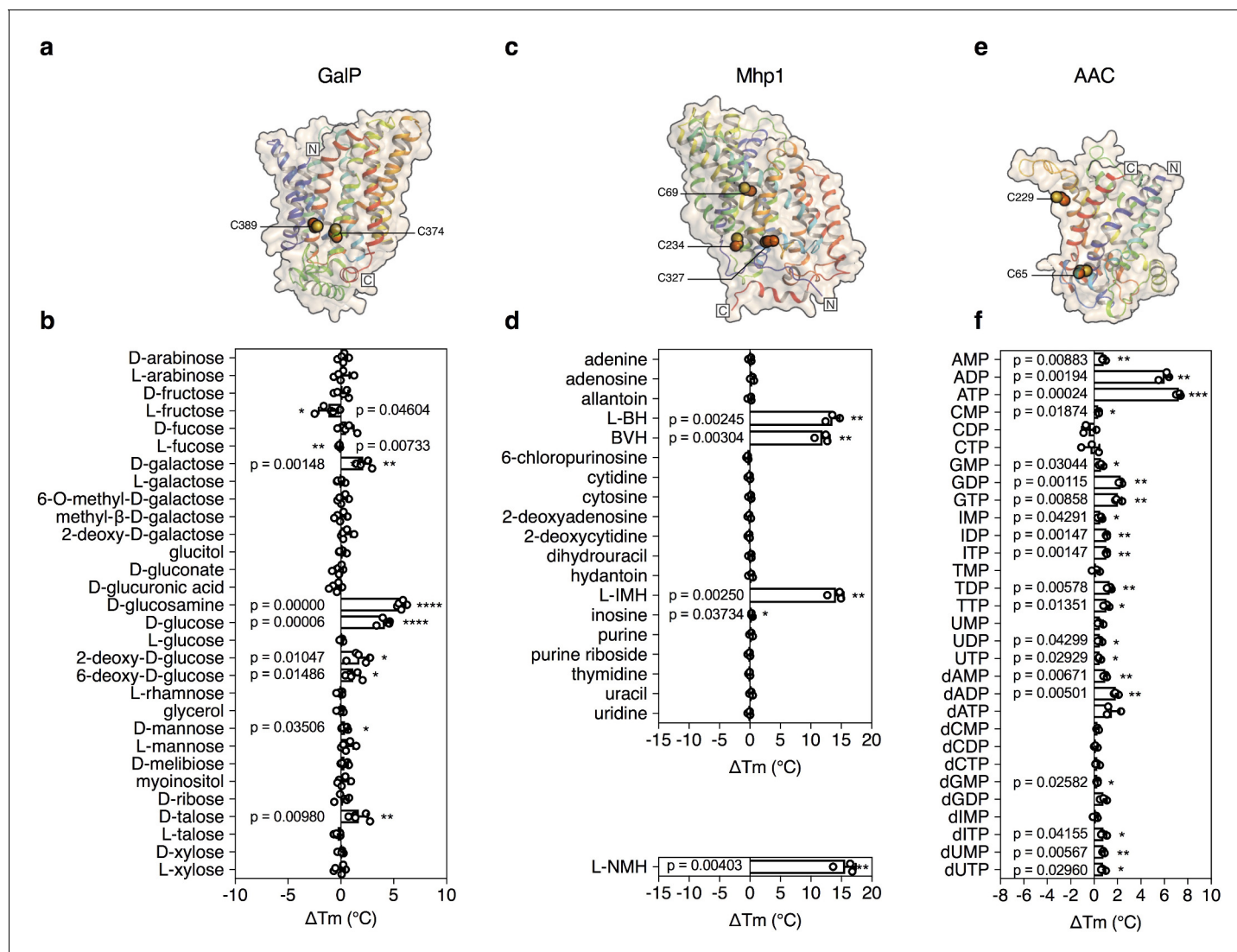


**Figure 2.** Validation of the method for determining substrate specificity using three unrelated proteins. (a), (c) and (e) Structural models of GalP (based on GLUT5, PDB 4YBQ), Mhp1 (PDB 2JLN) and AAC (based on Aac2p, PDB 4C9G), respectively. The models are shown in rainbow cartoon and wheat surface representations. Cysteine residues are shown as spheres, except for Cys-19 of GalP, which could not be modeled. (b), (d) and (f) Thermostability screen of GalP (3  $\mu\text{g}$ ), Mhp1 (3  $\mu\text{g}$ ) and AAC (2  $\mu\text{g}$ ) against sugar (50 mM final concentration), nucleobase (2 mM) and nucleotide libraries (2.5 mM), respectively. The temperature shift ( $\Delta T_m$ ) is the apparent melting temperature in the presence of compound minus the apparent melting temperature in the absence of compound. The data are represented by the standard deviation of five, three and three independent repeats, respectively. Two-tailed Student's *t*-tests assuming unequal variances were performed for the significance analysis (0.05 < *p*-value: not significant; 0.01 < *p*-value < 0.05: \*; 0.001 < *p*-value < 0.01: \*\*; 0.0001 < *p*-value < 0.001: \*\*\*; *p*-value < 0.0001: \*\*\*\*). L-BH, 5-benzyl-L-hydantoin; BVH, 5-bromovinylhydantoin; L-IMH, 5-indolylmethyl-L-hydantoin; L-NMH 5-(2-naphthylmethyl)-L-hydantoin.

DOI: <https://doi.org/10.7554/eLife.38821.004>

The following figure supplements are available for figure 2:

**Figure supplement 1.** Substrate-induced stabilization of the galactose transporter GalP.

DOI: <https://doi.org/10.7554/eLife.38821.005>

**Figure supplement 2.** Glucosamine is a transported substrate of the galactose transporter GalP.

DOI: <https://doi.org/10.7554/eLife.38821.006>

**Figure supplement 3.** Ligand-induced stabilization of Mhp1 in the presence of sodium ions.

DOI: <https://doi.org/10.7554/eLife.38821.007>

**Figure supplement 4.** Substrate screening of the mitochondrial ADP/ATP carrier.

DOI: <https://doi.org/10.7554/eLife.38821.008>

but with significantly smaller shifts (**Figure 2f**). For each type of nucleotide, the di- and tri-phosphate species showed larger shifts than the monophosphate forms, similar to the preference of ATP and ADP over AMP (**Figures 1d** and **2f**), showing that the assay can also identify functional groups that are important contributors to substrate binding.

### Substrate screening of a mitochondrial carrier from *Tetrahymena thermophila*

To see whether this method can be used to identify candidate substrates for a previously uncharacterized transporter, we performed a high-throughput screen on a purified mitochondrial carrier from the thermophilic ciliate *Tetrahymena thermophila* (UniProt I7M3J0). The carrier is phylogenetically related to the yeast mitochondrial carrier that transports inorganic phosphate in symport with a proton into the mitochondrial matrix for ATP synthesis (*Runswick et al., 1987*), but its substrates have not been identified experimentally. The population of carriers had an apparent  $T_m$  of  $56.0 \pm 0.8^\circ\text{C}$  and was screened against a library of 132 different mitochondrial compounds at pH 6.0 (**Figure 3**). The highest shift in the  $T_m$  of the population was observed for phosphate ( $\Delta T_m$ ;  $4.6 \pm 0.4^\circ\text{C}$ ), followed by glyoxylate ( $\Delta T_m$ ;  $3.6 \pm 0.8^\circ\text{C}$ ), acetyl-phosphate ( $\Delta T_m$ ;  $3.2 \pm 0.5^\circ\text{C}$ ) and phosphoenolpyruvate ( $\Delta T_m$ ;  $2.3 \pm 0.2^\circ\text{C}$ ) (**Figure 3—figure supplement 1**), whereas small shifts were observed for nucleotides. These compounds either contain phosphate as a functional group or resemble the structure of phosphate, such as glyoxylate (**Figure 3—figure supplement 2**). Thus, this assay can be used to narrow down substantially the number of potential substrate candidates from a library of unlabeled compounds. Uptake assays using protein reconstituted into proteoliposomes confirmed that the mitochondrial carrier exchanges phosphate (**Figure 3—figure supplement 3a**). We also tested whether glyoxylate, phosphoenolpyruvate and acetyl phosphate, which also gave a shift in thermostability assays, were transported, but none of them did (**Figure 3—figure supplement 3b**). However, in competition assays glyoxylate abolished uptake, demonstrating that it competes effectively with [ $^{33}\text{P}$ ]-orthophosphate for binding when present in a 1000-fold excess (**Figure 3—figure supplement 3c**).

### The effect of coupling ions

Secondary active transporters are widespread and often use the electrochemical gradient of protons or other ions to drive the uptake of substrates against their concentration gradient. Coupling ions are also recognized by transporters through specific interactions, often directly associated with the binding of substrates (*Kunji and Robinson, 2010; Krishnamurthy et al., 2009*).

5-Benzyl-L-hydantoin is transported by Mhp1 in symport with sodium ions (*Suzuki and Henderson, 2006; Shimamura et al., 2010*) and thus, we tested whether the temperature shifts of Mhp1 induced by substrate binding were ion-dependent. When different ions were tested, only sodium ions induced a large substrate stabilization, whereas relatively small stabilizations were observed in the presence of potassium, calcium and magnesium ions (**Figure 4a**).

Mitochondrial phosphate carriers are proton-driven, coupling phosphate translocation to proton symport (*Kunji and Robinson, 2010*). To investigate whether proton-dependency of substrate binding could be inferred from the assay, the shift in thermal stability by substrate binding was determined at pH 6.0 and 8.0. The pH can affect the reaction of maleimide groups of CPM with free thiols and the stability of the protein itself, but the  $\Delta T_m$  value shows the effect of pH on substrate binding only. In both cases, a substrate-induced stabilization was observed, but the effect was larger in pH 6.0 than in pH 8.0 ( $\Delta T_m$   $4.6 \pm 0.4^\circ\text{C}$  and  $2.6 \pm 0.4^\circ\text{C}$ , respectively) (**Figure 4b**).

As a control, we carried out the same experiment with the mitochondrial ADP/ATP carrier, which is not a proton symporter (**Figure 4c**). The opposite effect was observed; substrate binding at pH 8.0 led to a bigger thermostability shift than at pH 6.0. The predicted substrate-binding site of AAC has three positively charged residues that interact with the negatively charged phosphate groups of ADP and ATP (*Kunji and Robinson, 2006; Robinson and Kunji, 2006*). ATP has pKa values of 0.9, 1.5, 2.3 and 7.7, whereas ADP has pKa values 0.9, 2.8 and 6.8. This means that the substrates are more negatively charged at pH 8.0 compared to pH 6.0, which will enhance their binding to the positively charged residues of the substrate binding site, leading to an increase in thermostability. In the case of the phosphate carrier, the situation is very different. Phosphate has pKa values of 2.2, 7.2 and 12.3, and the predicted binding site contains two positively charged residues to neutralize the

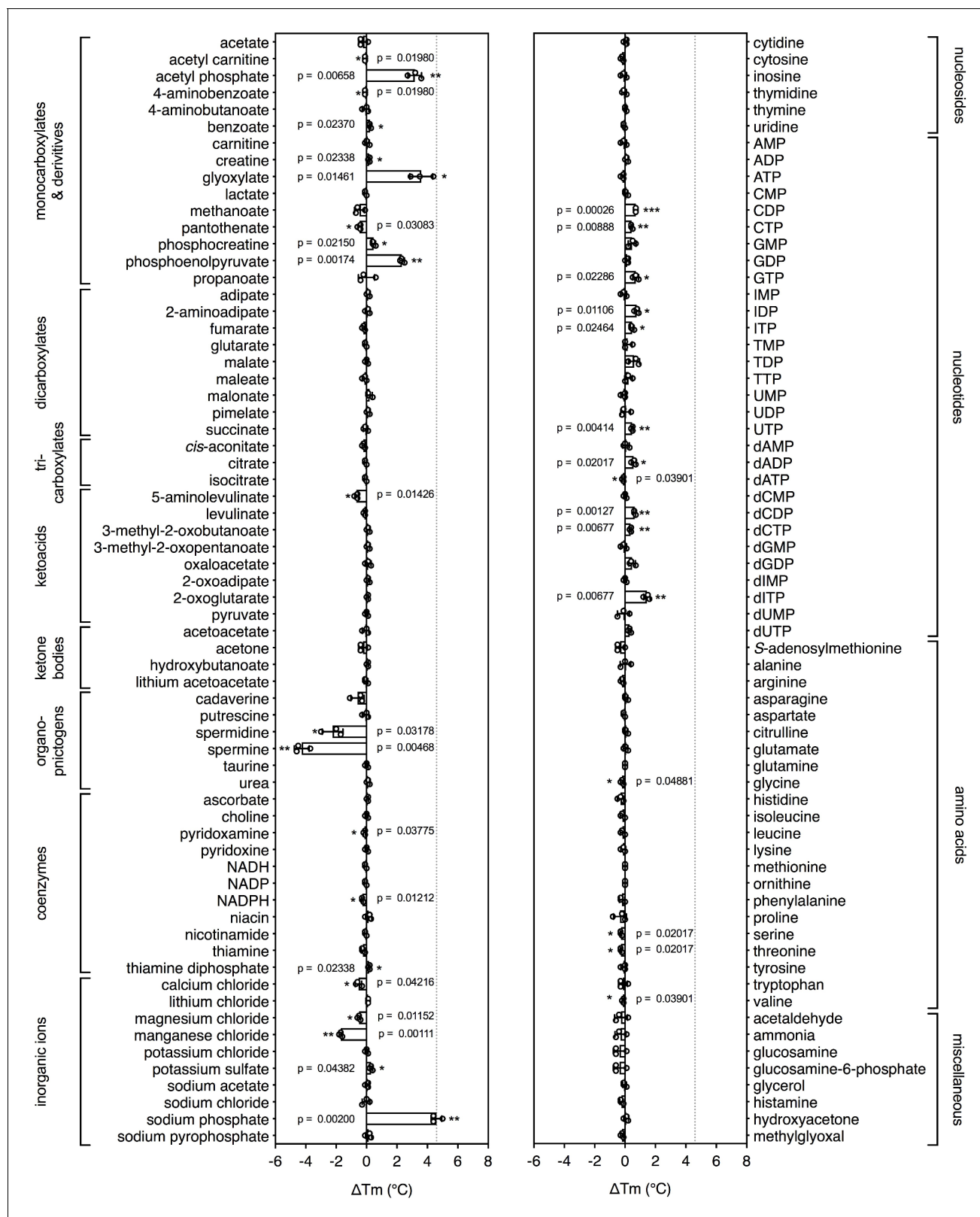


**Figure 3.** Identification of substrates for a mitochondrial phosphate carrier from the thermophilic ciliate *Tetrahymena thermophila*. Purified carrier (1  $\mu\text{g}$ ) in lauryl maltose neopentyl glycol was incubated at pH 6.0 with 2.5 mM of each library compound separately and the  $\Delta T_m$  was determined, which is the difference between the apparent melting temperatures in the presence and absence of the tested compound. The data are represented by the average and standard deviation of three independent assays. The significance tests were performed as described in the legend to **Figure 2**.  
 Figure 3 continued on next page

Figure 3 continued

DOI: <https://doi.org/10.7554/eLife.38821.009>

The following figure supplements are available for figure 3:

**Figure supplement 1.** Substrate-induced stabilization of the mitochondrial phosphate carrier.DOI: <https://doi.org/10.7554/eLife.38821.010>**Figure supplement 2.** Chemical structures of compounds that showed significant thermostability shifts with the mitochondrial phosphate carrier.DOI: <https://doi.org/10.7554/eLife.38821.011>**Figure supplement 3.** Phosphate is transported by the putative phosphate carrier of *Tetrahymena thermophila*.DOI: <https://doi.org/10.7554/eLife.38821.012>

two negative charges on phosphate. However, in addition, the binding site contains a negatively charged glutamate, which has a pKa of  $\sim 4.0$ . The coupling proton mediates bonding of the substrate and the carboxyl group of the glutamate residue (Kunji and Robinson, 2010), which occurs more readily at pH 6.0 than pH 8.0, explaining the difference in thermostability. In support of this notion the transport rates of the phosphate carrier are high at pH 6.0 and virtually absent at pH 8.0 (Stappen and Krämer, 1994). These results show that substrate binding stabilizes the transporters, but that this effect is enhanced further by the presence of coupling ions, providing testable hypotheses on energy coupling mechanisms.

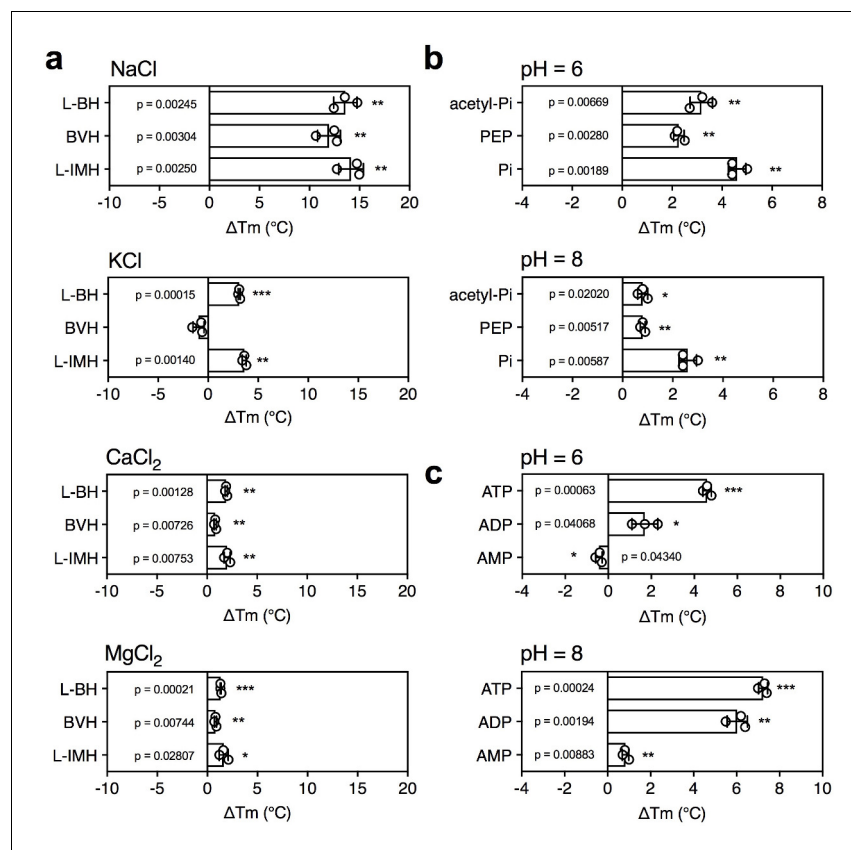


**Figure 4.** The effect of coupling ions on the stabilization of transporters by substrate binding. (a) Thermostability shifts of Mhp1 (3  $\mu$ g) induced by binding of hydantoin in the presence of 140 mM NaCl, KCl, CaCl<sub>2</sub> and MgCl<sub>2</sub>. L-BH: 5-benzyl-L-hydantoin, BVH: 5-bromovinylhydantoin, L-IMH: 5-indolmethyl-L-hydantoin. (b) Thermostability shifts of the phosphate carrier (1  $\mu$ g) induced by binding of 2.5 mM phosphate-containing compounds at pH 6.0 and 8.0. Acetyl-Pi: acetyl-phosphate, Pi: phosphate. (c) Thermostability shifts of the (2  $\mu$ g) induced by 2.5 mM ADP and ATP binding at pH 6.0 and 8.0, using AMP as control.

DOI: <https://doi.org/10.7554/eLife.38821.013>

## Discussion

We have shown that thermostability assays can be used to study the interaction of substrates with transporters, which is not intuitive, as substrates only bind transiently. Still, for diverse types of transport proteins, which differ in structure and transport mechanism, a shift in thermostability was observed in the presence of specific substrates. The shift is observed at concentrations well above the apparent  $K_m$  of transport, as under these conditions a larger part of the protein population is rescued from unfolding by binding of the substrate, increasing the overall number of interactions.

These studies highlight the different contributions that these assays can make to studying the properties of transport proteins. First, they can be used to limit the number of potential substrate candidates from libraries of unlabeled compounds, providing important clues about the substrate specificity (**Figures 2 and 3**). In the tested cases, the assay correctly identified the substrates from a set of chemically related compounds, including stereo-isomers. Still, these candidates need to be tested by transport or other types of assays, as the compounds could potentially be inhibitors, competitors or regulators. However, no prior knowledge is required and the number of radioactive compounds that need testing is highly reduced, meaning that it is easier and cheaper to establish a robust transport assay. Second, the assays can be used to extend the substrate specificity of known transport proteins, as was shown for GalP with D-glucosamine (**Figure 2b**). Third, they can be used to identify functional groups that are key to substrate binding, as shown for AAC, where nucleotide di- and tri-phosphates bound more tightly than nucleotide monophosphates (**Figure 2f**). In the case of mitochondrial phosphate carriers, the common properties of compounds, such as the phosphate group, may lead directly to the most probable candidates. Fourth, this assay can provide important clues on the involvement of coupling ions in substrate binding, as shown for cases where transport is driven by sodium ion or proton symport (**Figure 4**).

This method has major advantages over the traditional methods of identification. It is highly reproducible and can be performed in a high-throughput manner, allowing screening of about 100 compounds per machine per hour. The assay requires a relatively small amount of protein per assay (micrograms), depending on the number of buried cysteine residues. Another advantage is that the unfolding curves are themselves important quality checks, as they indicate that the protein is folded and therefore competent to bind substrate. Compounds which are poorly soluble in water can be added dissolved in dimethyl sulfoxide, provided that the final concentration of the solvent is kept low. Another advantage is that most compounds of the library can be used as internal controls, providing a reliable discrimination between positive and negative results. Furthermore, generic stabilizing and destabilizing compounds can be identified as more proteins of the same family are tested. For example, the polyamines spermine and spermidine have a destabilising effect on all purified mitochondrial carriers tested in our laboratory with the exception of AAC. These observations will reduce false positives for members of the same protein family. We have also observed that proteins incorporated into nanodiscs or amphipols can be successfully assayed using this approach, which is potentially useful for membrane proteins that are unstable in detergents.

There are also some limitations, as only proteins that have buried thiols can be used, although accessible cysteines can be tolerated as they only raise the base line of the assay without interfering with the unfolding curve. Thiol-containing compounds, such as cysteine or glutathione, cannot be screened as the probe reacts with them directly. However, changes in the fluorescence of environmentally sensitive dyes or endogenous tryptophans can be used as alternatives to CPM. Furthermore, the assay requires purified and stable transporter in detergent, although partially purified protein might be sufficient. Advances in bacterial (*King et al., 2016; Ward et al., 1999*), yeast (*Routledge et al., 2016*), insect (*Contreras-Gómez et al., 2014*), and mammalian (*Goehring et al., 2014; Andréll and Tate, 2013*) expression systems have allowed many transporters to be expressed in folded and functional states. Also, robust purification methods and novel classes of 'stabilizing' detergents, such as the neopentyl glycol maltoside detergents (*Chae et al., 2010*), have allowed even poorly expressed transporters to be purified in the small quantities required for these studies.

Even though the main purpose of this study was to identify potential substrates of transporters, the assays may also be used in drug discovery or in the identification of substrates, inhibitors and regulators of any other soluble or membrane proteins with occluded cysteines.

## Materials and methods

### Key resources table

Reagent type (species) or resource	Designation	Source or reference	Identifiers	Additional information
Chemical compound, drug	Dodecyl- $\beta$ -D-maltoside	Glycon Biochemicals GmbH	Glycon:D97002	
Chemical compound, drug	Dodecyl maltose neopentyl glycol	Anatrace	Anatrace:NG310	
Chemical compound, drug	N-[4-(7-diethylamino-4-methyl-3-coumarinyl)phenyl]maleimide (CPM)	Sigma	Sigma:C1484	
Chemical compound, drug	Complete Mini EDTA-free protease inhibitor tablets	Roche	Roche:5056489001	
Chemical compound, drug	Nickel Sepharose (High Performance)	GE Healthcare	GE Healthcare:17526802	
Chemical compound, drug	Nickel-NTA Superflow	Qiagen	Qiagen:30430	
Chemical compound, drug	Factor Xa protease	NEB	NEB:P8010L	
Chemical compound, drug	Tetraoleoyl cardiolipin (TOCL)	Avanti Polar Lipids	Avanti Polar Lipids:710335C	
Chemical compound, drug	<i>E. coli</i> polar lipid extract	Avanti Polar Lipids	Avanti Polar Lipids:100600C	
Chemical compound, drug	[ <sup>14</sup> C]-galactose	American Radiolabeled Chemicals	American Radiolabeled Chemicals:ARC0117	
Chemical compound, drug	[ <sup>14</sup> C]-glucosamine	American Radiolabeled Chemicals	American Radiolabeled Chemicals:ARC0118A	
Chemical compound, drug	[ <sup>33</sup> P]-orthophosphate	Hartmann Analytic	Hartmann Analytic:FF-01	
Chemical compound, drug	BioBeads	BioRad	BioRad:152–3920	
Chemical compound, drug	C10E5	Sigma	Sigma:76436	
Chemical compound, drug	Hydantoin compounds	Other		A gift from Marta Sans, Maria Kokkinidou and Arwen Pearson, University of Hamburg
Software, algorithm	Prism	GraphPad		
Strain, strain background ( <i>S. cerevisiae</i> )	<i>Saccharomyces cerevisiae</i> W303-1B	ATCC	ATCC:201238	
Strain, strain background ( <i>S. cerevisiae</i> )	<i>Saccharomyces cerevisiae</i> WB12	PMID:9878703		A gift from Dr H. Terada, Tokyo University of Science
Strain, strain background ( <i>E. coli</i> )	<i>Escherichia coli</i> JM1100	PMID:15558		
Recombinant DNA reagent	Modified pYES3 vector	PMID:26453935		

An additional key resources table is presented in **Supplementary file 2**, and details the compounds in the libraries.

### Materials

Chemicals were obtained from Sigma Aldrich and Thermo Fisher Scientific (USA). Nickel NTA and sepharose beads were purchased from Qiagen (USA). All enzymes were provided by New England BioLabs (USA). Lipids were purchased from Avanti Polar Lipids (USA) and detergents from Anatrace

(USA). The hydantoin compounds were a kind gift of Marta Sans, Maria Kokkinidou and Arwen Pearson (University of Hamburg).

### Protein expression

For expression of mitochondrial ADP/ATP carrier of *Thermothelomyces thermophila* and the putative phosphate carrier of *Tetrahymena thermophila* in yeast mitochondria, gene constructs were designed to contain an N-terminal tag composed of eight histidine residues followed by a Thr-Ser-Glu-Asp linker and an Ile-Glu-Gly-Arg Factor Xa protease cleavage site. The genes were cloned into pYES3/CT vector (Invitrogen, USA) with a constitutively active promoter (pMIR promoter of the *S. cerevisiae* phosphate carrier). The plasmids were transformed into *S. cerevisiae* WB.12 (MAT $\alpha$  ade2-1 trp1-1 ura3-1 can1-100 aac1::LEU2 aac2::HIS3) and W303-1B (MAT $\alpha$  leu2-3,112 trp1-1 can1-100 ura3-1 ade2-1 his3-11,15) strains, respectively. Cells were grown in a 50-l fermenter after which mitochondria were prepared (Kunji and Harding, 2003).

For expression of GalP in *E. coli* the promoter region and the *galP* gene, which was modified to encode six histidine residues at the C-terminus of the protein, were cloned into plasmid pBR322 to form plasmid pGP1, which was transformed into the galactose/glucose transport-deficient host strain JM1100 (*ptsG ptsM ptsF mgl galP Hfr  $\Delta$ his gnd thyA galK*) (Henderson et al., 1977). Cells were grown in basal salts medium supplemented with 30 mM glycerol, 20  $\mu$ g/ml thymine, 80  $\mu$ g/ml histidine and 15  $\mu$ g/ml tetracycline in a fermenter (30- or 100-liter scale). The gene *hyuP* from *M. liquefaciens*, modified to encode six histidine residues at the C-terminus, was cloned into plasmid pTTQ18 (Stark, 1987; Suzuki and Henderson, 2006). The His<sub>6</sub>-tagged Mhp1 hydantoin transport protein was expressed in *E. coli* BL21 (DE3) grown in M9 medium supplemented with 20 mM glycerol, 20 mM NH<sub>4</sub>Cl, 100  $\mu$ g/ml of carbenicillin, 0.2% w/v casamino acids, 2 mM MgSO<sub>4</sub>·7H<sub>2</sub>O, 0.4 mM CaCl<sub>2</sub>·2H<sub>2</sub>O, using induction by IPTG in 100-l fermenter cultures. In all cases after harvesting the intact cells preparations were made of inner membranes (Ward et al., 1999), which were stored at -80°C in Tris-HCl buffer pH 7.5 until used for purification of each individual protein.

### Protein purification

The mitochondrial ADP/ATP carrier and phosphate carrier were purified using the detergents dodecyl-maltoside and lauryl maltose neopentyl glycol, respectively, using established procedures (King et al., 2016).

For the purification of His-tagged GalP, *E. coli* membranes were solubilized in buffer containing 20 mM Tris-HCl pH 8, 20 mM imidazole, 300 mM NaCl, 20% glycerol and 1% dodecyl-maltoside for 1 hr at 4°C with gentle mixing to a final protein concentration of 2.5 mg/ml. After centrifugation (108,000 x g, 1 hr, 4°C), the supernatant was mixed with pre-washed nickel-NTA resin and purified by immobilized nickel affinity chromatography (1 ml resin per 37 mg of total protein; Superflow, Qia-gen) for batch-binding affinity chromatography for 1 hr at 4°C. Non-specific proteins were removed with buffer containing 20 mM Tris-HCl pH 8, 20 mM imidazole, 150 mM NaCl, 10% glycerol and 0.02% dodecyl-maltoside, after which His-tagged GalP was eluted with buffer containing 20 mM Tris-HCl pH 8, 200 mM imidazole, 100 mM NaCl, 5% glycerol and 0.02% dodecyl-maltoside. Imidazole was then removed by passing the sample through pre-equilibrated PD-10 desalting column (GE Healthcare). Protein samples were snap-frozen and stored in liquid nitrogen.

The purification of Mhp1 followed the same procedure as the GalP purification with the following modifications. Membranes were solubilized for 2 hr and incubated with Nickel NTA resin for 2 hr. The wash buffer contained 10 mM Tris-HCl pH 8, 20 mM imidazole, 10% glycerol and 0.05% dodecyl-maltoside and the elution buffer contained 10 mM Tris-HCl pH 8, 200 mM imidazole, 2.5% glycerol and 0.05% dodecyl-maltoside.

### Reconstitution

Twelve milligrams of total polar lipid extract (Avanti Polar Lipids, Alabaster) was dried under a stream of nitrogen, washed with methanol, and dried as before. Lipids were re-hydrated in 20 mM MES pH 6.5, 50 mM NaCl and, when required, compound was added to a final concentration of 20 mM from a 200 mM stock. Lipids were solubilised by vortexing in the presence of 1.5% (v/v) pentaethylene glycol monodecyl ether, and 50  $\mu$ g protein was added. The samples were incubated on ice for 5 min, and pentaethylene glycol monodecyl was removed to form liposomes by addition of bio-

beads (Bio-Rad, Hemel Hempstead, UK). Eight additions of bio-beads were made to the sample: the first four used 60 mg, and the final four used 120 mg. Between additions, the samples were incubated with inversion at 4°C for 20 min. Following the final bio-bead addition, the samples were incubated overnight at 4°C with inversion. Bio-beads were removed by passage of the sample through empty micro-bio spin columns (Bio-Rad, Hemel Hempstead, UK). The external buffer was replaced with 20 mM MES pH 6.5, 50 mM NaCl using a PD10 desalting column (GE Healthcare, Little Chalfont, UK). When required, competitors were added externally to a final concentration of 20 mM.

### Transport assays

Robotic transport assays were performed using a Hamilton MicroLab Star robot (Hamilton Robotics Ltd, UK). For GalP transport assays, *E. coli* cells (GalP-expressing strain pGP1/JM1100 and JM1100 control strains) were diluted to OD<sub>600</sub> of 20 in MES buffer (5 mM MES pH 6.6, 150 mM KCl) and incubated at room temperature with 20 mM glycerol for 10 min to be energized prior to being loaded into the wells of a MultiScreenHTS +Hi Flow-FB (pore size = 1.0 μm, Millipore). Transport assays were initiated by addition of 100 μl of buffer containing 5 μM [<sup>14</sup>C]-galactose (American Radiolabeled Chemicals, 0.2 GBq/mmol) or 5 μM [<sup>14</sup>C]-glucosamine (American Radiolabeled Chemicals, 0.2 GBq/mmol). For the competition assay, radiolabeled substrate was mixed with a 4000-fold excess of the competitor compound prior to the assay. For phosphate transport assays, 100 μl proteoliposomes were loaded into a MultiScreenHTS-HA 96-well filter plate (pore size, 0.45 μm; Millipore, Billerica), and transport was initiated by the addition of 100 μl of buffer containing 20 μM [<sup>33</sup>P]-orthophosphate (Hartmann Analytic, 0.5 GBq/mmol). For competition assays, transport was initiated in the presence of 20 mM compound (1000-fold excess). Transport was stopped after 0, 10, 20, 30, 45, 60, 150 s and, 5, 7.5 and 10 min incubation times with 200 μl ice-cold buffer and the samples were filtered and washed as above. Levels of radioactivity were measured by adding 200 μl MicroScint-20 (Perkin Elmer) and measured with a TopCount scintillation counter (Perkin Elmer). Initial rates were determined from the linear part of the uptake curves.

### Preparation of the mitochondrial compound library

To identify mitochondrial metabolites every enzyme in the KEGG metabolic database (Kanehisa *et al.*, 2017) was evaluated for mitochondrial localization using the MitoMiner database of mitochondrial localization evidence (Smith and Robinson, 2016). A wide range of data were considered including large-scale experimental evidence from GFP tagging and mass-spectrometry of mitochondrial fractions, mitochondrial targeting sequence predictions, immunofluorescent staining from the Human Protein Atlas (Thul *et al.*, 2017), and annotation from the Gene Ontology Consortium (The Gene Ontology Consortium, 2017). Ensembl Compara allowed these data to be shared across human, mouse, rat and yeast homologs (Zerbino *et al.*, 2018). Once a list of enzymes with probable mitochondrial localization was collated, KEGG was used to produce a corresponding list of potential mitochondrial compounds. Additional candidates were taken from a computer model of mitochondrial metabolism that manually partitioned metabolites on either side of the mitochondrial inner membrane (Smith and Robinson, 2011). Compounds were dissolved in PIPES buffer (10 mM PIPES pH 7.0, 50 mM NaCl) to a final concentration of 25 mM or in dimethyl sulfoxide to a final concentration of 100 mM. pH was adjusted if necessary and the stocks were frozen at –80°C.

### Analysis of the total number of identified transport protein substrates in different species

The TransportDB database contains a large number of organisms for which the transporter complement has been identified via a bioinformatic pipeline, along with substrate predictions for the transporters characterized (Elbourne *et al.*, 2017). To acquire the figures in **Supplementary file 1**, a Perl script driving an SQL query of the underlying MySQL database to TransportDB was developed to quantify those transporters where no prediction could be made for the substrate for the listed species. The number of transporters with unassigned specificity represents a minimal number, as the search procedure uses sequence similarity to characterised transporters as a criterion. However, the substrate specificity needs to be determined experimentally, as a single mutation in the binding site can profoundly change substrate recognition.

## Thermostability shift assay and library screening

To determine stability, purified protein (typically 1–3  $\mu\text{g}$ ) was mixed with 20  $\mu\text{g}/\text{ml}$  of the thiol-reactive fluorophore 7-diethylamino-3-(4'-maleimidylphenyl)-4-methylcoumarin (CPM) and the fluorescent intensity was measured over a 25–90°C range of temperature using a rotatory qPCR multi sample instrument (Rotor-Gene Q, Qiagen, the Netherlands). Following an initial 18°C pre-incubation step of 90 s, the temperature was ramped 1°C every 15 s, with a 4 s wait between readings, which is equal to a ramp rate of 5.6 °C/min. The excitation and emission wavelengths were 460 nm and 510 nm, respectively. Five mg/ml stocks of CPM prepared in dimethyl sulfoxide were diluted to 0.1 mg/ml and equilibrated in assay buffer for 1 hr at room temperature in the dark before addition to the protein sample. The assay buffer was usually the buffer in which the protein was purified or in a similar buffer with a different pH (MES for pH 6.0, HEPES for pH 8.0) or a different concentration of other ions. Data analyses and apparent melting temperatures ( $T_m$ , the inflection point of a melting temperature) were determined using software supplied with the instrument.

For GalP experiments, 500 mM sugar stocks were made in MilliQ water (Merck-Millipore, USA) as 10 times stocks. For Mhp1 experiments, 100 mM compound stocks were made in dimethyl sulfoxide as 50 times stocks.

## Data analyses and representation

Statistical analyses were performed using Microsoft Excel with the inbuilt function of two-tailed, two-sample unequal variance Student's *t*-test. The average apparent  $T_m$  of 'no ligand' control samples (three technical repeats within each Rotor-Gene Q run) was subtracted from the apparent  $T_m$  measured for each compound addition in the same run. This assay was performed with three or five biological repeats using independent batches of purified protein. The null hypothesis of the *t*-test was that the observed  $\Delta T_m$  for each compound was not significantly different from zero.

## Acknowledgements

This work was supported by grant MC\_UU\_00015/1 of the Medical Research Council, UK. HM gratefully acknowledges the Cambridge Commonwealth, European and International Trust for support of her PhD studies. PJFH thanks the Leverhulme Trust for an Emeritus Research Fellowship (Grant number EM-2014–045). The fermenters and allied equipment for protein production in Leeds were funded by the BBSRC (MPSI BBS/B/14418), the Wellcome Trust (JIF 062164/Z/00/Z) and the University of Leeds. The hydantoin derivatives were a kind gift from Marta Sans, Maria Kokkinidou and Arwen Pearson (University of Hamburg).

## Additional information

### Funding

Funder	Grant reference number	Author
Medical Research Council	MC_UU_00015/1	Homa Majd Martin S King Shane M Palmer Anthony C Smith Edmund RS Kunji
Cambridge Commonwealth, European and International Trust		Homa Majd
Leverhulme Trust	EM-2014 -045	Peter JF Henderson
Biotechnology and Biological Sciences Research Council	MPSI BBS/B/14418	David Sharples
Wellcome	JIF 062164/Z/00/Z	David Sharples
University of Leeds		David Sharples

The funders had no role in study design, data collection and interpretation, or the decision to submit the work for publication.

### Author contributions

Homa Majd, Martin S King, Conceptualization, Data curation, Formal analysis, Validation, Investigation, Visualization, Methodology, Writing—original draft, Writing—review and editing; Shane M Palmer, Resources, Large-scale Fermentation; Anthony C Smith, Resources, Data curation, Formal analysis; Liam DH Elbourne, Ian T Paulsen, Data curation, Software, Formal analysis; David Sharples, Resources, Methodology, Large-scale fermentation; Peter JF Henderson, Formal analysis, Supervision, Writing—original draft, Project administration, Writing—review and editing; Edmund RS Kunji, Conceptualization, Resources, Data curation, Formal analysis, Supervision, Funding acquisition, Validation, Investigation, Visualization, Methodology, Writing—original draft, Project administration, Writing—review and editing

### Author ORCIDs

Homa Majd  <http://orcid.org/0000-0002-2048-1839>

Martin S King  <http://orcid.org/0000-0001-6030-5154>

Peter JF Henderson  <http://orcid.org/0000-0002-9187-0938>

Edmund RS Kunji  <http://orcid.org/0000-0002-0610-4500>

### Decision letter and Author response

Decision letter <https://doi.org/10.7554/eLife.38821.020>

Author response <https://doi.org/10.7554/eLife.38821.021>

## Additional files

### Supplementary files

- Supplementary file 1. Current status of identification of transport proteins in different archaeal, eubacterial and eukaryotic species (April 2018).

DOI: <https://doi.org/10.7554/eLife.38821.014>

- Supplementary file 2. Key resources table.

DOI: <https://doi.org/10.7554/eLife.38821.015>

### Data availability

All data generated or analysed during this study are included in the manuscript and supporting files. Source data files have been provided in Dryad.

The following dataset was generated:

Author(s)	Year	Dataset title	Dataset URL	Database and Identifier
Majd H, King MS, Palmer SM, Smith AC, Elbourne LDH, Paulsen IT, Sharples D, Henderson PJF, Kunji ERS	2018	Data from: Screening of candidate substrates and coupling ions of transporters by thermostability shift assays	<a href="http://dx.doi.org/10.5061/dryad.532m1m8">http://dx.doi.org/10.5061/dryad.532m1m8</a>	Dryad Digital Repository, 10.5061/dryad.532m1m8

## References

- Andréll J, Tate CG. 2013. Overexpression of membrane proteins in mammalian cells for structural studies. *Molecular Membrane Biology* **30**:52–63. DOI: <https://doi.org/10.3109/09687688.2012.703703>, PMID: 22963530
- Calabrese AN, Jackson SM, Jones LN, Beckstein O, Heinkel F, Gsponer J, Sharples D, Sans M, Kokkinidou M, Pearson AR, Radford SE, Ashcroft AE, Henderson PJF. 2017. Topological dissection of the membrane transport protein Mhp1 derived from cysteine accessibility and mass spectrometry. *Analytical Chemistry* **89**:8844–8852. DOI: <https://doi.org/10.1021/acs.analchem.7b01310>, PMID: 28726379
- César-Razquin A, Snijder B, Frappier-Brinton T, Isserlin R, Gyimesi G, Bai X, Reithmeier RA, Hepworth D, Hediger MA, Edwards AM, Superti-Furga G. 2015. A call for systematic research on solute carriers. *Cell* **162**:478–487. DOI: <https://doi.org/10.1016/j.cell.2015.07.022>, PMID: 26232220

- Chae PS**, Rasmussen SG, Rana RR, Gotfryd K, Chandra R, Goren MA, Kruse AC, Nurva S, Loland CJ, Pierre Y, Drew D, Popot JL, Picot D, Fox BG, Guan L, Gether U, Byrne B, Kobilka B, Gellman SH. 2010. Maltose-neopentyl glycol (MNG) amphiphiles for solubilization, stabilization and crystallization of membrane proteins. *Nature Methods* **7**:1003–1008. DOI: <https://doi.org/10.1038/nmeth.1526>, PMID: 21037590
- Contreras-Gómez A**, Sánchez-Mirón A, García-Camacho F, Molina-Grima E, Chisti Y. 2014. Protein production using the baculovirus-insect cell expression system. *Biotechnology Progress* **30**:1–18. DOI: <https://doi.org/10.1002/btpr.1842>, PMID: 24265112
- Crichton PG**, Lee Y, Ruprecht JJ, Cerson E, Thangaratnarajah C, King MS, Kunji ER. 2015. Trends in thermostability provide information on the nature of substrate, inhibitor, and lipid interactions with mitochondrial carriers. *Journal of Biological Chemistry* **290**:8206–8217. DOI: <https://doi.org/10.1074/jbc.M114.616607>, PMID: 25653283
- Deng D**, Xu C, Sun P, Wu J, Yan C, Hu M, Yan N. 2014. Crystal structure of the human glucose transporter GLUT1. *Nature* **510**:121–125. DOI: <https://doi.org/10.1038/nature13306>, PMID: 24847886
- Deng D**, Sun P, Yan C, Ke M, Jiang X, Xiong L, Ren W, Hirata K, Yamamoto M, Fan S, Yan N. 2015. Molecular basis of ligand recognition and transport by glucose transporters. *Nature* **526**:391–396. DOI: <https://doi.org/10.1038/nature14655>, PMID: 26176916
- Elbourne LD**, Tetu SG, Hassan KA, Paulsen IT. 2017. TransportDB 2.0: a database for exploring membrane transporters in sequenced genomes from all domains of life. *Nucleic Acids Research* **45**:D320–D324. DOI: <https://doi.org/10.1093/nar/gkw1068>, PMID: 27899676
- Fauman EB**, Rai BK, Huang ES. 2011. Structure-based druggability assessment—identifying suitable targets for small molecule therapeutics. *Current Opinion in Chemical Biology* **15**:463–468. DOI: <https://doi.org/10.1016/j.cbpa.2011.05.020>, PMID: 21704549
- Goehring A**, Lee CH, Wang KH, Michel JC, Claxton DP, Bacongus I, Althoff T, Fischer S, Garcia KC, Gouaux E. 2014. Screening and large-scale expression of membrane proteins in mammalian cells for structural studies. *Nature Protocols* **9**:2574–2585. DOI: <https://doi.org/10.1038/nprot.2014.173>, PMID: 25299155
- Hediger MA**, Cléménçon B, Burrier RE, Bruford EA. 2013. The ABCs of membrane transporters in health and disease (SLC series): introduction. *Molecular Aspects of Medicine* **34**:95–107. DOI: <https://doi.org/10.1016/j.mam.2012.12.009>, PMID: 23506860
- Henderson PJ**. 1977. The multiplicity of components, energization mechanisms and functions involved in galactose transport into *Escherichia coli*. *Biochemical Society Transactions* **5**:25–28. DOI: <https://doi.org/10.1042/bst0050025>, PMID: 19320
- Henderson PJ**, Giddens RA, Jones-Mortimer MC. 1977. Transport of galactose, glucose and their molecular analogues by *Escherichia coli* K12. *Biochemical Journal* **162**:309–320. DOI: <https://doi.org/10.1042/bj1620309>, PMID: 15558
- Henderson PJ**, Maiden MC. 1990. Homologous sugar transport proteins in *Escherichia coli* and their relatives in both prokaryotes and eukaryotes. *Philosophical Transactions of the Royal Society B: Biological Sciences* **326**:391–410. DOI: <https://doi.org/10.1098/rstb.1990.0020>, PMID: 1970645
- Kanehisa M**, Furumichi M, Tanabe M, Sato Y, Morishima K. 2017. KEGG: new perspectives on genomes, pathways, diseases and drugs. *Nucleic Acids Research* **45**:D353–D361. DOI: <https://doi.org/10.1093/nar/gkw1092>, PMID: 27899662
- King MS**, Boes C, Kunji ER. 2015. Membrane protein expression in *Lactococcus lactis*. *Methods in enzymology* **556**:77–97. DOI: <https://doi.org/10.1016/bs.mie.2014.12.009>, PMID: 25857778
- King MS**, Kerr M, Crichton PG, Springett R, Kunji ERS. 2016. Formation of a cytoplasmic salt bridge network in the matrix state is a fundamental step in the transport mechanism of the mitochondrial ADP/ATP carrier. *Biochimica et Biophysica Acta (BBA) - Bioenergetics* **1857**:14–22. DOI: <https://doi.org/10.1016/j.bbabi.2015.09.013>, PMID: 26453935
- Krishnamurthy H**, Piscitelli CL, Gouaux E. 2009. Unlocking the molecular secrets of sodium-coupled transporters. *Nature* **459**:347–355. DOI: <https://doi.org/10.1038/nature08143>, PMID: 19458710
- Kunji ER**, Harding M. 2003. Projection structure of the atractyloside-inhibited mitochondrial ADP/ATP carrier of *Saccharomyces cerevisiae*. *Journal of Biological Chemistry* **278**:36985–36988. DOI: <https://doi.org/10.1074/jbc.C300304200>, PMID: 12893834
- Kunji ER**, Robinson AJ. 2006. The conserved substrate binding site of mitochondrial carriers. *Biochimica et Biophysica Acta (BBA) - Bioenergetics* **1757**:1237–1248. DOI: <https://doi.org/10.1016/j.bbabi.2006.03.021>, PMID: 16759636
- Kunji ER**, Robinson AJ. 2010. Coupling of proton and substrate translocation in the transport cycle of mitochondrial carriers. *Current Opinion in Structural Biology* **20**:440–447. DOI: <https://doi.org/10.1016/j.sbi.2010.06.004>, PMID: 20598524
- Kunji ERS**. 2012. Structural and Mechanistic Aspects of Mitochondrial Transport Proteins. In: Ferguson S (Ed). *Comprehensive Biophysics*. Elsevier.
- Lin L**, Yee SW, Kim RB, Giacomini KM. 2015. SLC transporters as therapeutic targets: emerging opportunities. *Nature Reviews Drug Discovery* **14**:543–560. DOI: <https://doi.org/10.1038/nrd4626>, PMID: 26111766
- McDonald TP**, Henderson PJ. 2001. Cysteine residues in the D-galactose-H<sup>+</sup> symport protein of *Escherichia coli*: effects of mutagenesis on transport, reaction with N-ethylmaleimide and antibiotic binding. *The Biochemical Journal* **353**:709–717. PMID: 11171069
- Mifsud J**, Ravaud S, Krammer EM, Chipot C, Kunji ER, Pebay-Peyroula E, Dehez F. 2013. The substrate specificity of the human ADP/ATP carrier AAC1. *Molecular Membrane Biology* **30**:160–168. DOI: <https://doi.org/10.3109/09687688.2012.745175>, PMID: 23173940

- Nomura N**, Verdon G, Kang HJ, Shimamura T, Nomura Y, Sonoda Y, Hussien SA, Qureshi AA, Coincon M, Sato Y, Abe H, Nakada-Nakura Y, Hino T, Arakawa T, Kusano-Arai O, Iwanari H, Murata T, Kobayashi T, Hamakubo T, Kasahara M, et al. 2015. Structure and mechanism of the mammalian fructose transporter GLUT5. *Nature* **526**:397–401. DOI: <https://doi.org/10.1038/nature14909>, PMID: 26416735
- Pao SS**, Paulsen IT, Saier MH. 1998. Major facilitator superfamily. *Microbiology and Molecular Biology Reviews* : **MMBR** **62**:1–34. PMID: 9529885
- Ramirez-Gaona M**, Marcu A, Pon A, Guo AC, Sajed T, Wishart NA, Karu N, Djoumbou Feunang Y, Arndt D, Wishart DS. 2017. YMDB 2.0: a significantly expanded version of the yeast metabolome database. *Nucleic Acids Research* **45**:D440–D445. DOI: <https://doi.org/10.1093/nar/gkw1058>, PMID: 27899612
- Rask-Andersen M**, Masuram S, Fredriksson R, Schiöth HB. 2013. Solute carriers as drug targets: current use, clinical trials and prospective. *Molecular Aspects of Medicine* **34**:702–710. DOI: <https://doi.org/10.1016/j.mam.2012.07.015>, PMID: 23506903
- Robinson AJ**, Kunji ER. 2006. Mitochondrial carriers in the cytoplasmic state have a common substrate binding site. *PNAS* **103**:2617–2622. DOI: <https://doi.org/10.1073/pnas.0509994103>, PMID: 16469842
- Routledge SJ**, Mikaliunaite L, Patel A, Clare M, Cartwright SP, Bawa Z, Wilks MD, Low F, Hardy D, Rothnie AJ, Bill RM. 2016. The synthesis of recombinant membrane proteins in yeast for structural studies. *Methods* **95**:26–37. DOI: <https://doi.org/10.1016/j.ymeth.2015.09.027>, PMID: 26431670
- Runswick MJ**, Powell SJ, Nyren P, Walker JE. 1987. Sequence of the bovine mitochondrial phosphate carrier protein: structural relationship to ADP/ATP translocase and the brown fat mitochondria uncoupling protein. *The EMBO Journal* **6**:1367–1373. DOI: <https://doi.org/10.1002/j.1460-2075.1987.tb02377.x>, PMID: 3038521
- Sajed T**, Marcu A, Ramirez M, Pon A, Guo AC, Knox C, Wilson M, Grant JR, Djoumbou Y, Wishart DS. 2016. ECMD 2.0: A richer resource for understanding the biochemistry of *E. coli*. *Nucleic Acids Research* **44**:D495–D501. DOI: <https://doi.org/10.1093/nar/gkv1060>, PMID: 26481353
- Shimamura T**, Weyand S, Beckstein O, Rutherford NG, Hadden JM, Sharples D, Sansom MS, Iwata S, Henderson PJ, Cameron AD. 2010. Molecular basis of alternating access membrane transport by the sodium-hydantoin transporter Mhp1. *Science* **328**:470–473. DOI: <https://doi.org/10.1126/science.1186303>, PMID: 20413494
- Simmons KJ**, Jackson SM, Brueckner F, Patching SG, Beckstein O, Ivanova E, Geng T, Weyand S, Drew D, Lanigan J, Sharples DJ, Sansom MS, Iwata S, Fishwick CW, Johnson AP, Cameron AD, Henderson PJ. 2014. Molecular mechanism of ligand recognition by membrane transport protein, Mhp1. *The EMBO Journal* **33**:1831–1844. DOI: <https://doi.org/10.15252/embj.201387557>, PMID: 24952894
- Smith AC**, Robinson AJ. 2011. A metabolic model of the mitochondrion and its use in modelling diseases of the tricarboxylic acid cycle. *BMC Systems Biology* **5**:102. DOI: <https://doi.org/10.1186/1752-0509-5-102>, PMID: 21714867
- Smith AC**, Robinson AJ. 2016. MitoMiner v3.1, an update on the mitochondrial proteomics database. *Nucleic Acids Research* **44**:D1258–D1261. DOI: <https://doi.org/10.1093/nar/gkv1001>, PMID: 26432830
- Stappen R**, Krämer R. 1994. Kinetic mechanism of phosphate/phosphate and phosphate/OH<sup>-</sup> antiports catalyzed by reconstituted phosphate carrier from beef heart mitochondria. *The Journal of Biological Chemistry* **269**:11240–11246. PMID: 8157653
- Stark MJ**. 1987. Multicopy expression vectors carrying the lac repressor gene for regulated high-level expression of genes in *Escherichia coli*. *Gene* **51**:255–267. DOI: [https://doi.org/10.1016/0378-1119\(87\)90314-3](https://doi.org/10.1016/0378-1119(87)90314-3), PMID: 3110013
- Suzuki S**, Henderson PJ. 2006. The hydantoin transport protein from *Microbacterium liquefaciens*. *Journal of Bacteriology* **188**:3329–3336. DOI: <https://doi.org/10.1128/JB.188.9.3329-3336.2006>, PMID: 16621827
- The Gene Ontology Consortium**. 2017. Expansion of the gene ontology knowledgebase and resources. *Nucleic Acids Research* **45**:D331–D338. DOI: <https://doi.org/10.1093/nar/gkw1108>, PMID: 27899567
- Thul PJ**, Åkesson L, Wiking M, Mahdessian D, Geladaki A, Ait Blal H, Alm T, Asplund A, Björk L, Breckels LM, Bäckström A, Danielsson F, Fagerberg L, Fall J, Gatto L, Gnann C, Hober S, Hjelmare M, Johansson F, Lee S, et al. 2017. A subcellular map of the human proteome. *Science* **356**:eaal3321. DOI: <https://doi.org/10.1126/science.aal3321>, PMID: 28495876
- Västermark Å**, Saier MH. 2014. Evolutionary relationship between 5+5 and 7+7 inverted repeat folds within the amino acid-polyamine-organocation superfamily. *Proteins: Structure, Function, and Bioinformatics* **82**:336–346. DOI: <https://doi.org/10.1002/prot.24401>, PMID: 24038584
- Walmsley AR**, Martin GE, Henderson PJ. 1994. 8-Anilino-1-naphthalenesulfonate is a fluorescent probe of conformational changes in the D-galactose-H<sup>+</sup> symport protein of *Escherichia coli*. *The Journal of Biological Chemistry* **269**:17009–17019. PMID: 8006005
- Ward A**, O'Reilly J, Rutherford NG, Ferguson SM, Hoyle CK, Palmer SL, Clough JL, Venter H, Xie H, Litherland GJ, Martin GE, Wood JM, Roberts PE, Groves MA, Liang WJ, Steel A, McKeown BJ, Henderson PJ. 1999. Expression of prokaryotic membrane transport proteins in *Escherichia coli*. *Biochemical Society Transactions* **27**:893–899. DOI: <https://doi.org/10.1042/bst0270893>, PMID: 10830123
- Wishart DS**, Jewison T, Guo AC, Wilson M, Knox C, Liu Y, Djoumbou Y, Mandal R, Aziat F, Dong E, Bouatra S, Sinelnikov I, Arndt D, Xia J, Liu P, Yallou F, Bjorn Dahl T, Perez-Pineiro R, Eisner R, Allen F, et al. 2013. HMDB 3.0—the human metabolome database in 2013. *Nucleic Acids Research* **41**:D801–D807. DOI: <https://doi.org/10.1093/nar/gks1065>, PMID: 23161693
- Yamashita A**, Singh SK, Kawate T, Jin Y, Gouaux E. 2005. Crystal structure of a bacterial homologue of Na<sup>+</sup>/Cl<sup>-</sup>-dependent neurotransmitter transporters. *Nature* **437**:215–223. DOI: <https://doi.org/10.1038/nature03978>, PMID: 16041361

- Yan N.** 2017. A glimpse of membrane transport through Structures-Advances in the structural biology of the GLUT glucose transporters. *Journal of Molecular Biology* **429**:2710–2725. DOI: <https://doi.org/10.1016/j.jmb.2017.07.009>, PMID: 28756087
- Zerbino DR,** Achuthan P, Akanni W, Amode MR, Barrell D, Bhai J, Billis K, Cummins C, Gall A, Girón CG, Gil L, Gordon L, Haggerty L, Haskell E, Hourlier T, Izuogu OG, Janacek SH, Juettemann T, To JK, Laird MR, et al. 2018. Ensembl 2018. *Nucleic Acids Research* **46**:D754–D761. DOI: <https://doi.org/10.1093/nar/gkx1098>, PMID: 29155950